

Theoretical Description of Time-Resolved Photoemission Spectroscopy: Application to Pump-Probe Experiments

J. K. Freericks,¹ H. R. Krishnamurthy,^{1,2,3} and Th. Pruschke⁴

¹*Department of Physics, Georgetown University, 37th and O Sts. NW, Washington, District of Columbia 20057, USA*

²*Centre for Condensed Matter Theory, Department of Physics, Indian Institute of Science, Bangalore 560012, India*

³*Condensed Matter Theory Unit, Jawaharlal Nehru Centre for Advanced Scientific Research, Bangalore 560064, India*

⁴*Institute for Theoretical Physics, University of Göttingen, Friedrich-Hund-Platz 1, D-37077 Göttingen, Germany*

(Received 29 June 2008; published 30 March 2009)

The theory for time-resolved, pump-probe, photoemission spectroscopy and other pump-probe experiments is developed. The formal development is completely general, incorporating all of the nonequilibrium effects of the pump pulse and the finite time width of the probe pulse, and including possibilities for taking into account band structure and matrix element effects, surface states, and the interaction of the photoexcited electrons with the system leading to corrections to the sudden approximation. We also illustrate the effects of windowing that arise from the finite width of the probe pulse in a simple model system by assuming the quasiequilibrium approximation.

DOI: 10.1103/PhysRevLett.102.136401

PACS numbers: 71.27.+a, 71.10.Fd, 71.30.+h, 79.60.-i

Pump-probe, femtosecond time-resolved (TR) photoemission spectroscopy (PES), and angle resolved PES (ARPES) techniques can examine the excited state nonequilibrium dynamics of electrons in solids [1], including some strongly correlated electron systems [2–4]. In these experiments, an intense pulse of radiation “pumps” the system into a highly excited nonequilibrium state. After a variable time delay, the system is subject to a weak “probe” pulse of higher energy photons, ejecting photoelectrons which are detected with energy (and angle) resolution.

Conventional (continuous probe beam) ARPES in layered materials can be well approximated [5] as a direct measure of the momentum and frequency dependent “lesser” Green’s function [6] of the electrons in the layers (i.e., their spectral function multiplied by the Fermi function). In more isotropic (three-dimensional) materials, the spectral function gets averaged over k_z , the component of the momentum perpendicular to the layers. The conventional interpretation of TR-PES is that the pump creates “hot electrons” in quasiequilibrium at a high “effective electronic temperature (T_{el})” compared to the lattice (phonons), which then cool gradually, so that the probe PES essentially measures equilibrium lesser functions at different values of T_{el} for different time delays between the pump and the probe pulses. For example, recent TR-ARPES experiments [3] on the layered material 1T-TaS₂ [believed to be an unusual, charge density wave (CDW)-induced, Mott insulator,] were interpreted in this way, using a dynamical mean-field theory (DMFT) [7] treatment of the 2- d Hubbard model for a range of temperatures and fillings, chosen as fitting parameters, for the different time delays used. Such an approach, while reasonable in many contexts, avoids addressing two important questions connected with (1) the nonequilibrium dynamical aspects of the experiment, and (2) the effects arising from the finite

width of the probe pulse (in the time domain). Here, we provide a theory that addresses all of these by extending the “one-step” treatment of continuous beam ARPES in equilibrium systems [8,9] to the present, nonequilibrium context.

We assume that the system, modeled by a quantum many-body Hamiltonian \mathcal{H} , is in equilibrium at a temperature T before the pump is turned on. It is represented in the distant past ($t \rightarrow -\infty$) by an ensemble of the (many-body) eigenstates $|\Psi_n\rangle$ of \mathcal{H} , present with the Boltzmann probability $\rho_n = Z^{-1} \exp[-E_n/(k_B T)]$ where E_n are the corresponding energy eigenvalues, and $Z = \sum_n \exp[-E_n/(k_B T)]$ is the partition function. Turning on the pump pulse modifies \mathcal{H} into a time-dependent Hamiltonian $\mathcal{H}_{\text{pump}}(t)$ whose precise form depends on the way one models the system and its interaction with the pump radiation [represented by the vector potential $\mathbf{A}_{\text{pump}}(\mathbf{r}, t)$ whose t dependence includes its turning on and off]. Then, at time t_0 , just before the probe is turned on, the system is represented by the ensemble of states $|\Psi_n^I(t_0)\rangle \equiv U(t_0, -\infty)|\Psi_n\rangle$ (with the same Boltzmann probability as above), where $U(t', t) \equiv \mathcal{T}_t \{ \exp[-i \int_t^{t'} dt_1 \mathcal{H}_{\text{pump}}(t_1)/\hbar] \}$ is the unitary time development operator of the system in the presence of the pump radiation. Here, \mathcal{T}_t is the time ordering operator and $\{|\Psi_n^I(t_0)\rangle\}$ acts as the ensemble of “initial” states for the quantum transitions generated by the probe pulse.

Similarly, when the probe is turned on, the Hamiltonian is modified to $\mathcal{H}_{\text{pump}}(t) + \mathcal{H}_{\text{probe}}(t)$ to appropriately include the effects of the probe pulse. A particular “initial” state $|\Psi_n^I(t_0)\rangle$ therefore evolves at any later time t to the “final” state $|\Psi_n^F(t)\rangle \equiv \hat{U}(t, t_0)|\Psi_n^I(t_0)\rangle$, where $\hat{U}(t, t_0) \equiv \mathcal{T}_t \exp[-i \int_{t_0}^t dt_1 \{ \mathcal{H}_{\text{pump}}(t_1) + \mathcal{H}_{\text{probe}}(t_1) \} / \hbar]$ is the full time development operator in the presence of the probe (and pump) pulse. If we have nonoverlapping pump and probe pulses, $\mathcal{H}_{\text{pump}}(t_1) = \mathcal{H}$ for $t_1 > t_0$.

We model the photocurrent operator representing the detector, designed to detect photoelectrons of momentum \mathbf{k} around \mathbf{k}_e and placed at a macroscopic distance \mathbf{R}_d outside the sample, as $\mathbf{J}_d \simeq (\hbar \mathbf{k}_e / m_e) c_{\mathbf{k}_e; \mathbf{R}_d}^\dagger c_{\mathbf{k}_e; \mathbf{R}_d}$ where $c_{\mathbf{k}_e; \mathbf{R}_d}^\dagger$ creates an electron in a wave-packet state with a momentum space wave function $\phi_{\mathbf{k}_e; \mathbf{R}_d}(\mathbf{k})$ which is sharply peaked at \mathbf{k}_e , but is nevertheless localized in real space around \mathbf{R}_d . The measured photocurrent at time t is then $\langle \mathbf{J}_d \rangle(t) = \sum_n \rho_n \langle \Psi_n^F(t) | \mathbf{J}_d | \Psi_n^F(t) \rangle$.

Typically, the pump pulse is so intense that it needs to be treated nonperturbatively, but the probe pulse is weak enough that $\mathcal{H}_{\text{probe}}(t)$ can be treated by perturbation theory. Hence, to leading order

$$\hat{U}(t, t_0) \simeq U(t, t_0) - \frac{i}{\hbar} \int_{t_0}^t dt_1 U(t, t_1) \mathcal{H}_{\text{probe}}(t_1) U(t_1, t_0). \quad (1)$$

We assume the photons in the pump radiation have energies smaller than the work function W of the sample and do not photoemit. (This also makes it reasonable to treat the pump vector potential as classical, and use the Peierls' substitution when low-energy electrons have a tight binding band structure.) Hence, the photoemission process arises only from the second term in Eq. (1). The leading contribution to the measured photocurrent is of second order [10] in $\mathcal{H}_{\text{probe}}(t)$, and using Eq. (1) and the properties of U , we obtain

$$\begin{aligned} \langle \mathbf{J}_d \rangle(t) &= \frac{1}{(\hbar)^2} \int_{t_0}^t dt_2 \int_{t_0}^{t_2} dt_1 \langle U(-\infty, t_2) \mathcal{H}_{\text{probe}}(t_2) U(t_2, t) \\ &\quad \times \mathbf{J}_d U(t, t_1) \mathcal{H}_{\text{probe}}(t_1) U(t_1, -\infty) \rangle_{\mathcal{H}}; \\ \langle O \rangle_{\mathcal{H}} &\equiv \sum_n \rho_n \langle \Psi_n | O | \Psi_n \rangle = Z^{-1} \text{Tr}[e^{-\mathcal{H}/(k_B T)} O]. \quad (2) \end{aligned}$$

Let $c_{\nu \mathbf{k}_\parallel}^\dagger$ create an electron in an eigenstate of the one-electron (e.g., LDA) band structure Hamiltonian \mathcal{H}_0 appropriate to the sample with the surface [11], with energy $\epsilon_{\nu \mathbf{k}_\parallel}$. We assume a flat surface (the x - y plane) so that the eigenstates can be labeled by \mathbf{k}_\parallel , the wave vector component parallel to the surface, and another index or quantum number ν , which can, in principle, include surface states as well. Then, the component of $\mathcal{H}_{\text{probe}}(t_1)$ corresponding to the absorption of a photon of momentum $\hbar \mathbf{q}$ (frequency $\omega_q = cq$ and annihilation operator a_q) is [12]

$$\sum_{\nu, \nu', \mathbf{k}_\parallel} s(t_1) e^{-i\omega_q t_1} M_q(\nu, \nu'; \mathbf{k}_\parallel) c_{\nu' \mathbf{k}_\parallel + \mathbf{q}_\parallel}^\dagger c_{\nu \mathbf{k}_\parallel} a_q. \quad (3)$$

Here, for simplicity, we have dropped the spin indices of the electron operators. The probe pulse shape function, $s(t)$, describes the temporal profile of the probe pulse, including its turning on and off. M is the one-electron matrix element $\langle \nu' \mathbf{k}'_\parallel | [ie\hbar \mathbf{A}_{\text{probe}}(\mathbf{r})/m_e c] \cdot \nabla | \nu \mathbf{k}_\parallel \rangle$, where $\mathbf{A}_{\text{probe}}(\mathbf{r}) \equiv \mathbf{A}_q(\mathbf{r}) \exp(i\mathbf{q} \cdot \mathbf{r})$, with the slowly varying $\mathbf{A}_q(\mathbf{r})$ describing the spatial profile of the probe pulse [including its attenuation as it traverses the sample].

Conservation of momentum components parallel to the surface requires $\mathbf{k}'_\parallel = \mathbf{k}_\parallel + \mathbf{q}_\parallel$, while the detailed properties of M depend on the modeling of the sample, especially its surface [13]. Note that this choice of the one-electron basis of \mathcal{H}_0 is just convenient for representing $\mathcal{H}_{\text{probe}}(t)$; all many-body and nonequilibrium effects are incorporated in our expressions for the photocurrent derived below.

The terms in Eq. (3) can excite an electron from an occupied level ($\nu \mathbf{k}_\parallel$) inside the system to a high-energy band level ($\nu' \mathbf{k}'_\parallel$). When $\epsilon_{\nu' \mathbf{k}'_\parallel} - \mu$, where μ is the chemical potential, exceeds W , a so-called time-reversed LEED (or TRL) state [11] is created, that has a wave function component outside the sample which is an outgoing plane wave of wave vector $\mathbf{k}'(\nu') \equiv [\mathbf{k}'_\parallel, k'_z(\nu')]$, with ν' and k'_z related by the condition $\epsilon_{\nu' \mathbf{k}'_\parallel} - \mu = (\hbar k')^2 / (2m_e) + W$. This electron is detectable as a photoelectron outside the sample, with momentum $\hbar \mathbf{k}'$ unless inelastic collisions within the sample reduce its kinetic energy. These processes can be taken into account as follows. The wave-packet state for the detected photoelectron has exactly the same component in the TRL state $|\nu' \mathbf{k}'_\parallel\rangle$ as in the plane wave state $|\mathbf{k}'(\nu')\rangle$. Hence, $c_{\mathbf{k}_e; \mathbf{R}_d}^\dagger = \sum_{\nu', \mathbf{k}'_\parallel} \phi_{\mathbf{k}_e; \mathbf{R}_d}(\mathbf{k}'(\nu')) c_{\nu' \mathbf{k}'_\parallel}^\dagger$. Using this and Eqs. (2) and (3), we find

$$\begin{aligned} \langle \mathbf{J}_d \rangle(t) &= \frac{\hbar \mathbf{k}_e}{m_e} \sum_{\nu, \nu', \mathbf{k}_\parallel, \mathbf{k}'_\parallel} \phi_{\mathbf{k}_e; \mathbf{R}_d}^*[\mathbf{k}(\nu)] \phi_{\mathbf{k}_e; \mathbf{R}_d}[\mathbf{k}'(\nu')] P(t); \\ P(t) &\equiv \frac{1}{(\hbar)^2} \sum_{\nu_1, \nu'_1, \mathbf{k}_{\parallel 1}} \sum_{\nu_2, \nu'_2, \mathbf{k}_{\parallel 2}} M_q^*(\nu_2, \nu'_2, \mathbf{k}_{\parallel 2}) M_q(\nu_1, \nu'_1, \mathbf{k}_{\parallel 1}) \\ &\quad \times \int_{t_0}^t dt_2 \int_{t_0}^{t_2} dt_1 s(t_2) s(t_1) e^{i\omega_q(t_2 - t_1)} \langle c_{\nu_2 \mathbf{k}_{\parallel 2}}^\dagger(t_2) \\ &\quad \times c_{\nu'_2 \mathbf{k}_{\parallel 2} + \mathbf{q}_\parallel}(t_2) c_{\nu \mathbf{k}_\parallel}^\dagger(t) c_{\nu' \mathbf{k}_\parallel + \mathbf{q}_\parallel}(t_1) \\ &\quad \times c_{\nu_1 \mathbf{k}_{\parallel 1}}(t_1) \rangle_{\mathcal{H}}. \quad (4) \end{aligned}$$

Here, $c_{\nu'_1 \mathbf{k}_{\parallel 1}}^\dagger(t_1)$, $c_{\nu \mathbf{k}_\parallel}(t)$, etc., are the electron creation and destruction operators in the Heisenberg picture appropriate to $\mathcal{H}_{\text{pump}}(t)$:

$$\begin{aligned} c_{\nu'_1 \mathbf{k}_{\parallel 1}}^\dagger(t_1) &\equiv U(-\infty, t_1) c_{\nu'_1 \mathbf{k}_{\parallel 1}}^\dagger U(t_1, -\infty), \\ c_{\nu \mathbf{k}_\parallel}(t) &\equiv U(-\infty, t) c_{\nu \mathbf{k}_\parallel} U(t, -\infty), \text{ etc.}, \quad (5) \end{aligned}$$

and for simplicity of notation, we have not shown all the variables that P depends on. Equation (4), the central new result of this Letter, is a formally exact expression for the measured pump-probe photocurrent, in terms of a nonequilibrium, contour-ordered, three-particle Green's function [14] on the Kadanoff-Baym-Keldysh contour in the complex time plane going from $-\infty$ to t back to $-\infty$, with t_1 on the outward real contour and t_2 on the return real contour [15]. In practical calculations, e.g., using DMFT, a third contour down the imaginary axis to $-i\beta$ is often needed in order to evaluate the relevant operator averages.

In many experimentally relevant contexts, it is reasonable to assume that the high-energy TRL state electrons photoexcited by the probe interact weakly with the other degrees of freedom in the sample, their dynamics being

primarily determined by an effective (e.g., LDA) band Hamiltonian \mathcal{H}_0 because their energy is far removed from the Fermi level. In that case, one can approximate the expectation value in Eq. (4) as the factorized product

$$\begin{aligned} & \langle c_{\nu_2 \mathbf{k}_{\parallel 2}}^\dagger(t_2) c_{\nu_1 \mathbf{k}_{\parallel 1}}(t_1) \rangle_{\mathcal{H}} \langle c_{\nu_2' \mathbf{k}_{\parallel 2} + \mathbf{q}_{\parallel}}(t_2) c_{\nu_1' \mathbf{k}_{\parallel 1}}^\dagger(t) \rangle_{\mathcal{H}_0} \langle c_{\nu \mathbf{k}_{\parallel}}(t) c_{\nu_1' \mathbf{k}_{\parallel 1} + \mathbf{q}_{\parallel}}^\dagger(t_1) \rangle_{\mathcal{H}_0} \\ & = \langle c_{\nu_2 \mathbf{k}_{\parallel 2}}^\dagger(t_2) c_{\nu_1 \mathbf{k}_{\parallel 1}}(t_1) \rangle_{\mathcal{H}} \delta_{\nu_2', \nu'} \delta_{\nu_1', \nu} \delta_{\mathbf{k}_{\parallel 2} + \mathbf{q}_{\parallel}, \mathbf{k}_{\parallel 1}'} \delta_{\mathbf{k}_{\parallel 1} + \mathbf{q}_{\parallel}, \mathbf{k}_{\parallel}} e^{i[(\epsilon_{\nu_1' \mathbf{k}_{\parallel 1}} - \mu)(t-t_2) - (\epsilon_{\nu \mathbf{k}_{\parallel}} - \mu)(t-t_1)]}, \end{aligned} \quad (6)$$

where the expectation values of the electron creation and annihilation operators in the high-energy states are evaluated with respect to the single-particle Hamiltonian \mathcal{H}_0 (and hence can be factorized and evaluated using Wick's theorem), but the low-energy states are evaluated with respect to \mathcal{H} . We can further simplify this by neglecting the \mathbf{k} widths of $\phi_{\mathbf{k}_e, \mathbf{R}_d}(\mathbf{k})$, whence $\mathbf{k}(\nu) \simeq \mathbf{k}'(\nu') \simeq \mathbf{k}_e$, and $\nu = \nu' = \nu_e$ such that $\epsilon_{\nu_e \mathbf{k}_{e\parallel}} - \mu = (\hbar k_e)^2 / (2m_e) + W \equiv \hbar\omega_{\mathbf{q}} - \hbar\omega$, with $\hbar\omega$ being the excitation energy remaining in the system after the photoemission process. Furthermore, photon wave-vectors are orders of magnitude smaller than the electron wave vectors, and can be ignored. Hence, we obtain

$$P(t) \simeq -i \frac{1}{(\hbar)^2} \sum_{\nu_1, \nu_2} M_{\mathbf{q}}^*(\nu_2, \nu_e; \mathbf{k}_{e\parallel}) M_{\mathbf{q}}(\nu_1, \nu_e; \mathbf{k}_{e\parallel}) \int_{t_0}^t dt_2 \int_{t_0}^{t_2} dt_1 s(t_2) s(t_1) e^{i\omega(t_2-t_1)} G_{\nu_1 \mathbf{k}_{e\parallel}, \nu_2 \mathbf{k}_{e\parallel}}^<(t_1, t_2), \quad (7)$$

where $G^<$ is the well-known two-time (nonequilibrium) lesser Green's function [6] given by

$$G_{\nu_1 \mathbf{k}_{e\parallel}, \nu_2 \mathbf{k}_{e\parallel}}^<(t_1, t_2) \equiv i \langle c_{\nu_2 \mathbf{k}_{e\parallel}}^\dagger(t_2) c_{\nu_1 \mathbf{k}_{e\parallel}}(t_1) \rangle_{\mathcal{H}}. \quad (8)$$

The dominant contribution to $P(t)$ in Eq. (7) ultimately comes from quantum numbers ν_1 and ν_2 corresponding to the low-energy bands near the Fermi level, extending up to the bands that electrons get excited into by the pump laser. As we show elsewhere [16], the result in Eq. (7) can also be obtained using a scattering description of the photoemission process and invoking the sudden approximation. But the treatment presented above, leading to Eq. (4), is much more general, and permits, in principle, processes that are neglected in the sudden approximation.

In the traditional context of a continuous probe beam ARPES for a sample in equilibrium, $G^<(t_1, t_2)$ is only a function of $(t_1 - t_2)$ and $s(t) = 1$. In this case, $P(t)$ diverges for large $(t - t_0)$, and is better interpreted in terms of a constant rate of detection of photoelectrons proportional to $\lim_{t \rightarrow \infty} \lim_{t_0 \rightarrow -\infty} P(t)/(t - t_0)$, given by $-i \sum_{\nu_1, \nu_2} M_{\mathbf{q}}^*(\nu_2, \nu_e; \mathbf{k}_{e\parallel}) M_{\mathbf{q}}(\nu_1, \nu_e; \mathbf{k}_{e\parallel}) \tilde{G}_{\nu_1 \mathbf{k}_{e\parallel}, \nu_2 \mathbf{k}_{e\parallel}}^<(\omega)$ where the tilde denotes a Fourier transform (FT) to the frequency representation. Furthermore, in a clean, highly anisotropic, layered system where all the electrons that are photoexcited arise from one band, and surface states and matrix element effects can be ignored, the ν labels can be dropped, whence this rate is proportional to $-i \tilde{G}_{\mathbf{k}_{e\parallel}}^<(\omega) = A_{\mathbf{k}_{e\parallel}}(\omega) f(\omega)$ which is the standard result [5]. However, the formalism developed above contains all the ingredients necessary to go beyond this.

Next, we explore the consequences of the finite width of the probe pulse envelope $s(t)$ in the context of a material that can be well approximated by the $d \rightarrow \infty$ Hubbard model, for which the DMFT is exact [7]. Here, electrons hop with amplitude $t_{\text{Hub}}^*/2\sqrt{d}$ (t_{Hub}^* set equal to 1, and serving as the unit of energy in the following discussion)

between nearest-neighbor sites on an infinite dimensional ($d \rightarrow \infty$) hypercubic lattice, and two electrons on the same site with opposite spin have a repulsive energy U . We consider only TR-PES, i.e., the angle integrated P , $\langle P \rangle_{\hat{k}_e}$, and approximate the matrix element M [13] as a constant. We also use the quasiequilibrium approximation. Then, $\langle P \rangle_{\hat{k}_e}$ is calculable as the frequency domain convolution

$$\lim_{t \rightarrow \infty} \lim_{t_0 \rightarrow -\infty} \langle P \rangle_{\hat{k}_e} = -i \int d\nu \tilde{G}^<(\omega - \nu) |\tilde{s}(\nu)|^2 / 2\pi \quad (9)$$

where $\tilde{s}(\nu)$ is the FT of $s(t)$, and $\tilde{G}^<(\omega)$ is the equilibrium, local lesser Green's function at temperature T_{el} .

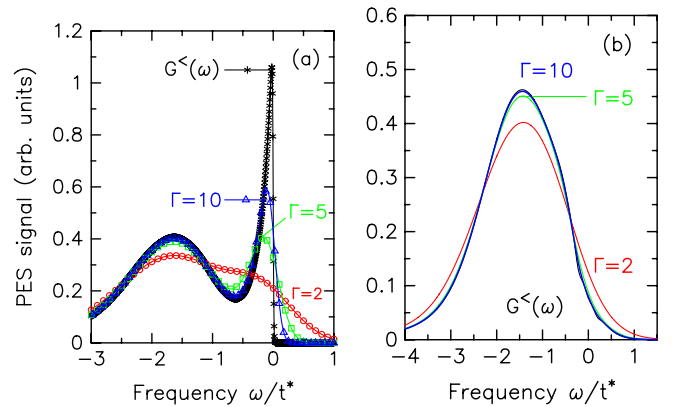


FIG. 1 (color online). Photoemission spectra at half-filling with $U = 3$. The temperatures are $T = 0.00539$ for panel (a) and $T = 0.0189$ for panel (b). The continuous beam photoemission curve is in black and is labeled by $G^<(\omega)$, while the pump-probe curves for different probe widths are in other colors and labeled by their widths Γ . In panel (a), symbols are used to differentiate the different curves. In panel (b), the curves with $\Gamma = 10$ and the lesser Green's function are essentially indistinguishable except for some kinks near $\omega = 0$. The $\Gamma = 5$ curve has a slightly lower peak, but then merges with the others, while the $\Gamma = 2$ curve is clearly distinguished.

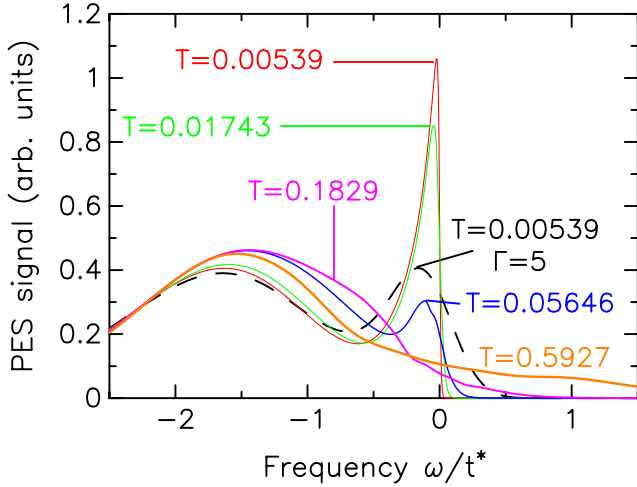


FIG. 2 (color online). Time-resolved photoemission spectra at half filling with $U = 3$ ($\Gamma = 5$) at temperatures $T = 0.00539$ (dashed line) versus the equilibrium continuous beam PES at different T s. Note how the windowing effect is different from thermal broadening effects, especially for positive energies.

We work at half filling and solve the DMFT problem using the numerical renormalization group [17] for the retarded Green's function with standard procedures [7,17]. We take the shape function $s(t)$ to be a Gaussian $s(t) = \exp[-(t - \bar{t})^2/\Gamma^2]/(\Gamma\sqrt{\pi})$ with a varying width Γ and pump-probe time delay \bar{t} (which sets T_{e1}). Our PES signals are normalized so that the integrated weight in all spectra are identical.

In Fig. 1, we compare the continuous beam PES [$s(t) = 1$] with the pump-probe PES for varying Γ , for $U = 3$ corresponding to a strongly correlated metal. Coarse high-energy features of the spectra are determined reasonably well for $\Gamma \gtrsim 5$, but sharp features like the quasiparticle peak require much larger Γ to be accurately captured. In Fig. 2, where we compare the metallic PES for $T = 0.00539$ and $\Gamma = 5$ (dashed line) with the continuous beam PES for various temperatures, we see that the spectral shape due to the broadening effect of a finite probe pulse width is qualitatively different from that due to thermal broadening. The high temperatures needed to broaden the quasiparticle peak to the same extent as the windowing effect also generate higher energy upper Hubbard band contributions that the windowing effect alone does not.

In conclusion, we have developed a formally exact many-body theory for pump-probe TR-ARPES that also takes into account two new effects: (i) the nonequilibrium dynamics induced by the intense pump pulse and (ii) the windowing effect due to the finite width of the probe pulse. Under simplifying assumptions the PES signal including all the nonequilibrium effects can be represented in terms of integrals of the lesser Green's function in the presence of the pump pulse. The broadening effect from the windowing can make it difficult to extract sharp spectral features unless the pulse width is wide enough in the time domain.

This effect is qualitatively different from the broadening caused by raising T .

J. K. F. acknowledges support from the National Science Foundation under Grant No. DMR-0705266. H. R. K. is supported under ARO Grant No. W911NF0710576 with funds from the DARPA OLE Program, and from the Department of Science and Technology, India. Th. P. acknowledges support from the collaborative research center (SFB) 602. We also acknowledge useful discussions with T. Devereaux, M. Grioni, G.-H. Gweon, B. Moritz, L. Perfetti, and K. Rossnagel.

- [1] E.g., see A.L. Cavalieri *et al.*, *Nature (London)* **449**, 1029 (2007); M. Lisowski *et al.*, *Phys. Rev. Lett.* **95**, 137402 (2005), and references therein.
- [2] L. Perfetti *et al.*, *Phys. Rev. Lett.* **99**, 197001 (2007).
- [3] L. Perfetti *et al.*, *Phys. Rev. Lett.* **97**, 067402 (2006); *New J. Phys.* **10**, 053019 (2008).
- [4] F. Schmitt *et al.*, *Science* **321**, 1649 (2008).
- [5] J.C. Campuzano, M.R. Norman, and M. Randeria, in *Physics of Superconductors*, edited by K.H. Bennemann and J.B. Ketterson (Springer, Berlin, 2004), Vol. II, pp. 167–273; A. Damascelli, Z. Hussain, and Z.-X. Shen, *Rev. Mod. Phys.* **75**, 473 (2003).
- [6] L.P. Kadanoff and G. Baym, *Quantum Statistical Mechanics* (Benjamin, New York, 1962).
- [7] A. Georges *et al.*, *Rev. Mod. Phys.* **68**, 13 (1996).
- [8] W.L. Schaich and N.W. Ashcroft, *Phys. Rev. B* **3**, 2452 (1971).
- [9] For a recent review and other references, see C.-O. Almbladh, *J. Phys. Conf. Ser.* **35**, 127 (2006).
- [10] This is because $\mathcal{H}_{\text{probe}}$ is linear in the photon creation or destruction operators [see Eq. (3)], and we need them to be paired together to get a nonzero expectation value. Note that we have not exhibited the photon Hamiltonian or states explicitly, but do take their effects into account.
- [11] N. Stojic *et al.*, *Phys. Rev. B* **77**, 195116 (2008).
- [12] Equation (3) plus its Hermitian conjugate summed over all \mathbf{q} , ν' , ν , and \mathbf{k}_{\parallel} is an exact representation for $\mathcal{H}_{\text{probe}}$.
- [13] For calculations of M in simple model contexts, see Ref. [8], and for a recent *ab initio* band structure calculation, see Ref. [11].
- [14] Jørgen Rammer, *Quantum Field Theory of Non-equilibrium States* (Cambridge University Press, Cambridge, 2007).
- [15] Analogous arguments show that the time-resolved linear response (after pumping) at time t of an operator \mathcal{A} to a general pulsed perturbation $\int_0^t dt_1 s(t_1) \mathcal{B}$ is given by the standard expression $\delta\langle \mathcal{A} \rangle_t = \int_{-\infty}^{\infty} \chi_{\mathcal{A}\mathcal{B}}^{\text{ret}}(t, t') s(t') dt'$, where χ is the retarded, two-time, nonequilibrium, Keldysh contour susceptibility in the presence of the pump pulse, given by $(-i/\hbar)\langle \mathcal{A}(t)\mathcal{B}(t') - \mathcal{B}(t')\mathcal{A}(t) \rangle_{\mathcal{H}} \theta(t - t')$. For a recent study in the context of time-resolved optical spectroscopy, see M. Eckstein and M. Kollar, *Phys. Rev. B* **78**, 205119 (2008).
- [16] J. K. Freericks *et al.*, arXiv:0809.2347 [*Phys. Status Solidi B* (to be published)].
- [17] R. Bulla, T. A. Costi, and Th. Pruschke, *Rev. Mod. Phys.* **80**, 395 (2008), and references therein.